ELSEVIER

Ceramics International 28 (2002) 37–41

CERAMICS INTERNATIONAL

www.elsevier.com/locate/ceramint

# Functionally graded Ti/HAP coatings on Ti–6Al–4V obtained by chemical solution deposition

Yong-Mu Lim[a], Yeong-Joon Park[b], Yeon-Hum Yun[c], Kyu-Seog Hwang[b,d,*]

[a]*Department of Ophthalmic Optics, Kwangju Health College, 638-8 Shinchang-dong, Kwangsan-ku, Kwangju 506-306, South Korea*
[b]*Department of Dental Materials and Dental Materials Research Institute, School of Dentistry, Chonnam National University, 5 Hak 1-dong, Dong-ku, Kwangju 501-190, South Korea*
[c]*Department of Mineral and Energy Resources Engineering, Chonnam National University, 300 Yongbong-dong, Buk-gu, Kwangju 500-757, South Korea*
[d]*School of Automotive and Mechanical Engineering, Nambu University, 864-1 Wolgye-dong, Kwangsan-ku, Kwangju 506-302, South Korea*

Received 19 March 2001; received in revised form 30 March 2001; accepted 25 April 2001

## Abstract

Graded $Ti_{100-x}/HAP_x$ ($x=0-100\%$) films were prepared on Ti–6Al–4V implants by chemical solution deposition using a titanium-isopropoxide chelated by acetylacetone, calcium nitrate and phosphoric acid as starting materials. Ti/HAP solutions with variable HAP contents from 0 to 100% at 10% intervals were spin coated on the substrates and prefired at 500 °C. X-ray diffraction and field emission-scanning electron microscope analysis showed that Ti/HAP coatings were obtained with a dense interface between coating and substrate by final annealing at 500 °C and higher. The effectiveness of the functionally graded HAP/Ti coatings was discussed based on the analysis of the variation of Ca and P contents in simulated body fluid as a function of annealing temperature. © 2002 Elsevier Science Ltd and Techna S.r.l. All rights reserved.

*Keywords:* $Ti_{100-x}/HAP_x$; Chemical solution deposition; Simulated body fluid

## 1. Introduction

The bioceramic hydroxyapatite [$Ca_{10}(PO_4)_6(OH)_2$, HAP] has attracted widespread interest because of its orthopaedic and tissue bioactivity properties [1,2]. On implantation, HAP can bind tightly to the surrounding bone tissue, because its chemical and crystallographic structures are very similar to those of human bone [3]. However, mechanical limitations prevent implants made from HAP alone. As a result, nearly all bone and tooth implants are presently made from metal alloys, which have a higher durability and strength than bulk HAP.

Among metallic implants, the Ti–6Al–4V alloy is widely used to manufacture implants because of its excellent mechanical properties with a tensile strength of 860 MPa and yield strength of 795 MPa, and its low specific gravity of 4.5 g/cm$^3$ [4]. However, Ti-based alloys may not be the best from a biological point of view since they may somewhat corrode when implanted.

If HAP is applied as coating on Ti-based alloys, its advantages can be properly exploited. The concept of coating metal implant surfaces with HAP combines the mechanical benefits of metal alloys with the biocompatibility of HAP [5,6]. For this reason, HAP is used as a suitable coating material to achieve strong early fixation of uncemented prostheses.

Various coating techniques such as plasma spraying, electrochemical deposition and chemical solution deposition (CSD) are presently under development to achieve suitable properties for biomedical applications [7–10]. Commercial, HAP coatings, which are commonly produced by plasma spraying, have been shown to exhibit clinical problems such as delamination, leading to premature wear and loosening of implants [11]. Although, to improve adhesion between coatings and implants, new synthetic approaches are currently being developed, there has been little information on the increase of bonding strength.

In order to solve this problem, we studied compositionally graded HAP structures. The present work is focused on the application by CSD of a functionally graded Ti/HAP intermediate layer as a bond coat for HAP.

---

[*] Corresponding author at second address. Tel.: +82-62-970-0150; fax: +82-62-972-6200.
*E-mail address:* khwang@mail.nambu.ac.kr (K.-S. Hwang).

PII: S0272-8842(01)00055-4

## 2. Experimental procedure

HAP sols were used as precursors, derived from calcium nitrate [$Ca(NO_3)_2 \cdot 4H_2O$] and phosphoric acid ($H_3PO_4$) dissolved in ethylene glycol monomethyl ether ($CH_3OCH_2CH_2OH$). The molar ratio of Ca:P in the sol was set to 1.67:1. Since the titanium alkoxide used in this study is very unstable in air, to prepare a chelated Ti sol, acetylacetone (2.4-pentanedione) and water were mixed into titanium (IV) isopropoxide {$Ti[OCH(CH_3)_2]_4$} dissolved in isopropanol. Ti/HAP coating solutions with variable HAP concentrations between 0 and 100% at 10% intervals were fabricated by mixing HAP sol and chelated Ti sol. This mixed solution was diluted with isopropanol and ethylene glycol monomethyl ether to achieve an appropriate viscosity for deposition of smooth films by spin coating (viscosity: 3 cps). Fig. 1 shows the experimental procedure.

Ti–6Al–4V was selected as a substrate. This substrate was ultrasonically cleaned in $H_2O_2$, mirror polished with an autopolisher, and finally rinsed in ethanol.

The starting solution (100% Ti–0% HAP) was initially spin coated onto Ti–6Al–4V substrates ($2\ \mathrm{cm}^{\Phi} \times 0.2^{t}$) at 3500 rpm for 5 s and as-coated films were dried at 150 °C for 15 min. The dried films were pyrolyzed at 500 °C for 5 min in order to burn out organics. To prepare functionally graded $Ti_{100-x}/HAP_x$ coatings, spin coating and pyrolysis were orderly repeated with decreasing Ti and increasing HAP contents at 10% intervals. Finally, the prefired films were annealed at 500, 600, 700 and 800 °C for 30 min in argon.

The crystalline structure and graded composition of annealed films were evaluated by X-ray diffraction analysis (XRD) (D-Max-1200, Rigaku Co.) utilizing Cu*K*α radiation. The surface morphology and composition of cross-sections of films were evaluated by field emission-scanning electron microscopy (FE-SEM) (S-4700, Hitachi Co.) in conjunction with an energy dispersive X-ray spectrometry (EDX) using a Robinson-type back-scattered electron detector.

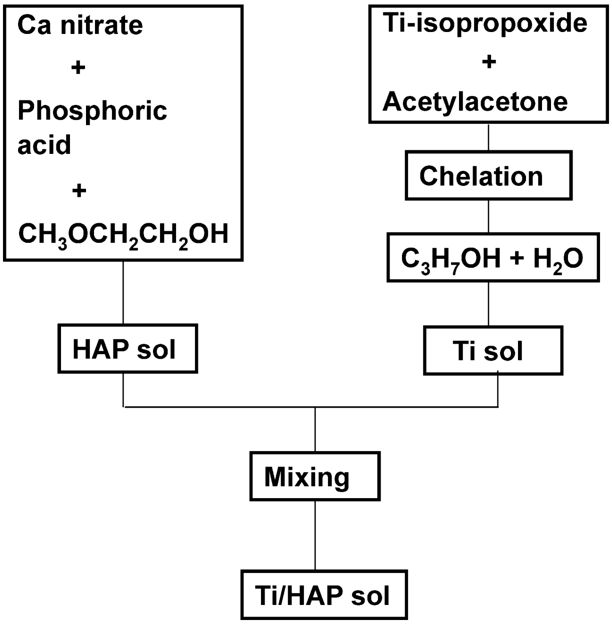

Fig. 1. Schematic diagram of the process to prepare Ti/HAP films.

The in vitro formation of HAP in annealed films was evaluated by immersing the films in a simulated body fluid (SBF). The SBF was prepared by dissolving NaCl, $NaHCO_3$, KCl, $K_2HPO_4 \cdot 3H_2O$, $MgCl_2 \cdot 6H_2O$, $CaCl_2$ and $Na_2SO_4$ in deionized distilled water. To this solution, 50 mM Tris–(hydroxymethyl) aminomethane [$(CH_2OH)_3CNH_2$] and 45 mM hydrochloric acid (HCl) were used as buffering agents to maintain the pH of SBF at 7.25 at 36.5 °C [12]. The reagent grade chemicals used and their concentrations for the preparation of SBF are shown in Table 1. Five samples per annealing temperature were immersed in 20 ml of SBF for 14 days. The experiments were performed in a constant temperature-circulating bath (Model 90, Poly Science Co.) at a temperature of 36.5 °C. After soaking, the samples were removed from the SBF, carefully rinsed with distilled water, and dried at room temperature.

The variation of the crystallinity of the incubated samples was investigated by XRD. Since it is difficult to separate HAP newly formed biomimetically after incubation from the annealed HAP film, we investigated the change of ion concentration of the SBF as a function of the incubation time by Inductively Coupled Plasma-atomic emission spectrometry (ICP) (JY38 plus, Jobin Yvon Co.).

## 3. Results and discussion

Fig. 2 shows the film morphology (a) and the EDX results (b) across a Ti/HAP coating on a Ti–6Al–4V implant. The Ti content decreased gradually with increasing distance from the substrate. Conversely, the Ca and P contents increased with increasing distance from the substrate; the more distant from the substrate the lower the Ca and P contents. This means that films were successfully formed with functional gradation. The

Table 1
Reagents for preparing the SBF

| Adding order | Reagent | Amount g/l $H_2O$ |
|---|---|---|
| 1 | $(CH_2OH)_3CNH_2$ | 6.005 |
| 2 | NaCl | 7.995 |
| 3 | $NaHCO_3$ | 0.353 |
| 4 | KCl | 0.224 |
| 5 | $K_2HPO_43H_2O$ | 0.228 |
| 6 | $MgCl_26H_2O$ | 0.305 |
| 7 | $CaCl_22H_2O$ | 0.368 |
| 8 | $Na_2SO_4$ | 0.071 |
| 9 | 2mol/l HCl | 20 ml |

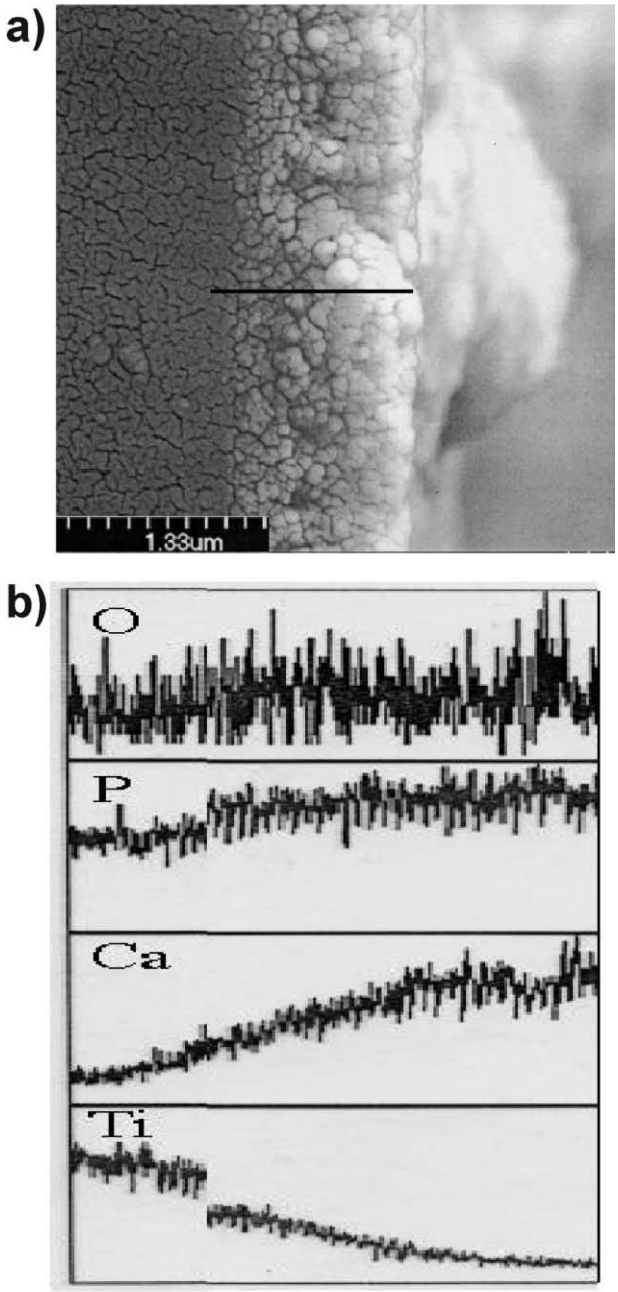

Fig. 2. Cross-sectional variation of compositions of Ti/HAP films annealed at 500 °C.

cross-sectional surface of the film was dense and a clear interface boundary between the film and the substrate could not be recognized. This suggests that the bond between the film and the substrate is sufficiently strong. Further, it is noted that grain growth of HAP may be suppressed by Ti, resulting in small grain size in the lower part of the coating. However, in the upper part, grain growth of HAP was observed, probably due to sufficient supply of Ca and P.

Fig. 3 shows the surface morphologies of Ti/HAP coatings annealed at 500 (a) and 800 °C (b), respectively. The surface of the film annealed at 500 °C was porous with plate-like grains thoughout the film, as shown in Fig. 3(a). The film annealed at 800 °C showed well-crystallized phases. However, after annealing at high temperature [see Fig. 3(b)], some pores were observed in the film. This may be attributed to the effects of shrinkage in the gel coating on annealing.

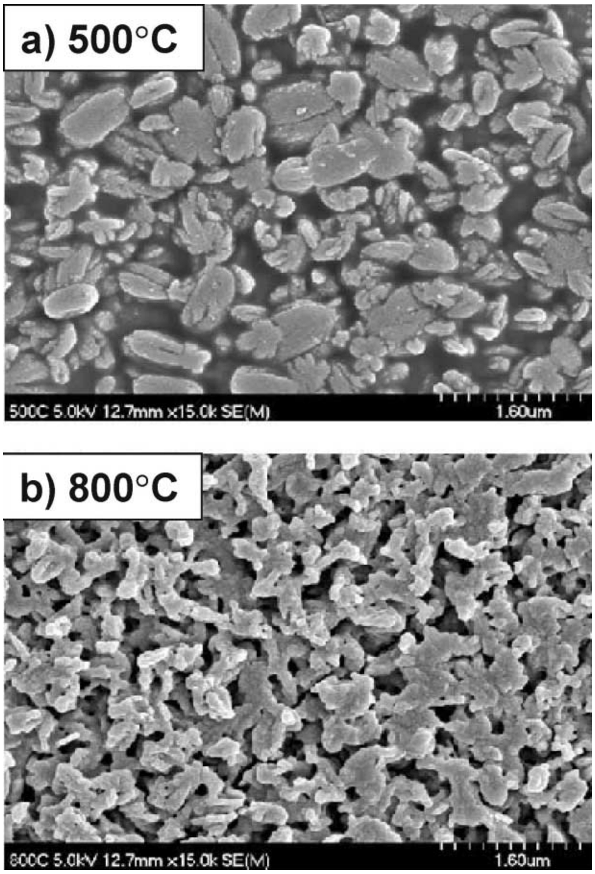

Fig. 3. Surface morphologies of Ti/HAP films annealed at (a) 500 and (b) 800 °C.

Fig. 4 shows the XRD patterns of functionally graded films annealed at 500, 600, 700 and 800 °C, respectively. In film annealed at 500 °C, the HAP structure started to become visible with peaks corresponding to the (002), (210), (211), (112), (300) and (202). After annealing at higher temperature, the films became more crystalline. This implies that annealing is very effective to form well-crystallized HAP. Neither β-tricalcium phosphate [$Ca_3(PO_4)_2$] (β-TCP) phase, corresponding to the decomposition of carbonated HAP (CHA) at high temperature, nor other phases, such as $TiO_2$ due to the Ti oxidation, were detected in the coating.

Fig. 5 shows the XRD pattern of functionally graded Ti/HAP coatings annealed at 500 (a), 600 (b), 700 (c) and 800 °C (d), respectively, after incubation in SBF for 14 days. Since it is difficult to compare the differences of HAP peak intensities, we defined the degree of HAP intensity ($\alpha$) as follows:

$\alpha(\%) = I_{\mathrm{HAP}(211)}/I_{\mathrm{Ti}(101)}$

where $I_{\mathrm{HAP}(211)}$ and $I_{\mathrm{Ti}(101)}$ are the intensities of HAP (211) which is the strongest peak of the powder diffraction pattern, and Ti (101) reflections which is the strongest peak among the peaks corresponding to substrate used, respectively. As shown in Table 2, with increasing the incubation time to 14 days, the HAP peak intensities slightly increased in all samples, probably due to secondary biomimetic HAP formation in SBF. This indicates that the number of active sites for HAP nucleation on the functionally graded Ti/HAP coatings increased. Generally, HAP formation from an aqueous solution is controlled by nucleation and crystal growth. Nucleation under normal condition is possible only when the solution is supersaturated with respect to HAP [13]. In such an environment, once HAP nuclei are formed, they can grow spontaneously by consuming Ca and P ions from the surrounding fluid.

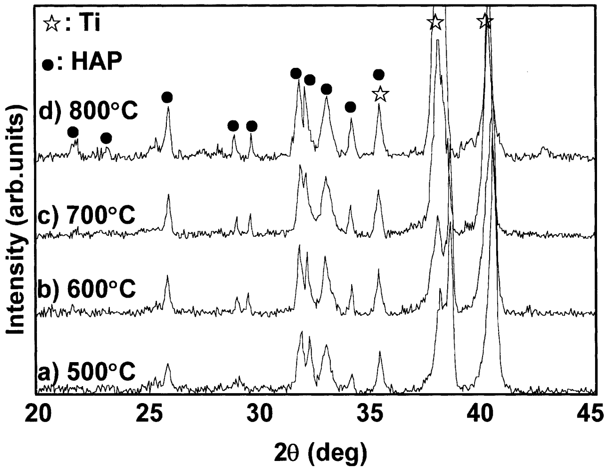

Fig. 4. XRD pattern of Ti/HAP films annealed at various temperatures.

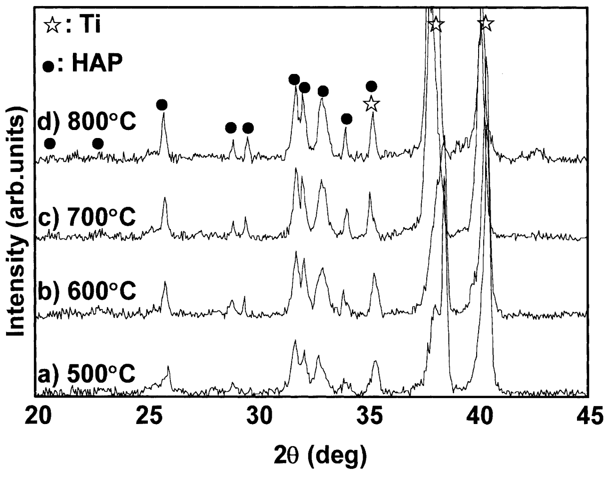

Fig. 5. XRD patterns of Ti/HAP films annealed at various temperatures after incubation in SBF for 14 days.

In view of this, in order to confirm the variation of Ca and P contents in SBF as a function of the annealing temperatures, we performed ICP analyses on the SBF after incubation. Variation of P and Ca contents of the soaking solutions is shown in Figs. 6 and 7. P and Ca concentrations decreased gradually with increasing incubation time, indicating that the amount of HAP formed on the coatings increased. However, films annealed at higher temperatures resulted in a lower relative decrease of concentrations. The lowest contents of P and Ca were observed for films annealed at 500 °C. We assume that pores and incompletely crystallized phases in the film annealed at lower temperature may offer more sites for attachments of Ca and P ions, since, from the surface observation by SEM, films annealed at low temperature (500 °C) showed a porous and plate-like structure [see Fig. 3(a)]. In future investigations, the optimal annealing condition leading to high mechanical strength must be evaluated more clearly on the basis of a bonding test between the coating and the implant.

We have confirmed that graded films prepared by HAP variation with 10% intervals are responsible for biomimetic HAP formation. At present, most coatings prepared on Ti implants designed to combine the mechanical benefits of metal with the biocompatibility

Table 2
Relative peak intensity (α) of HAP films annealed at various temperatures

| | Temperature (°C) | | | |
|---|---|---|---|---|
| Time (day) | 500 | 600 | 700 | 800 |
| 0 | 20.9 | 25.0 | 27.2 | 37.0 |
| 14 | 23.4 | 25.9 | 28.9 | 40.7 |

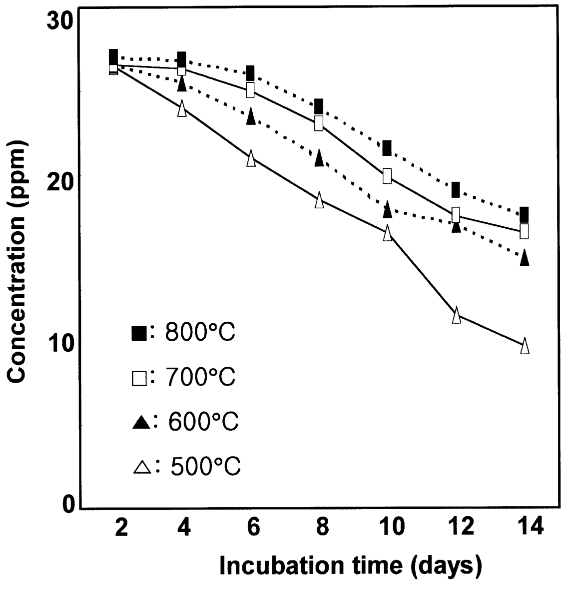

Fig. 6. Variation of P concentration in SBF as a function of incubation time of films annealed at various temperatures.

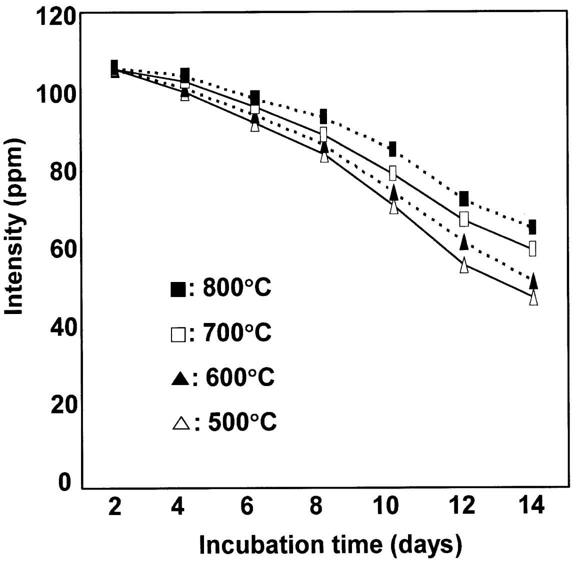

Fig. 7. Variation of Ca concentration in SBF as a function of incubation time of films annealed at various temperatures.

of HAP exhibited short-comings during long-term application due to different composition between ceramic and metal. From our microscopical, structural and in vitro results, it can be concluded that preparation of functionally graded Ti/HAP coatings was successfully achieved. However, further research is needed to test the mechanical strength and to carry out in vivo evaluations of the coatings.

## 4. Conclusions

Graded $Ti_{100-x}/HAP_x$ ($x=0$ – 100%) films were prepared on Ti–6Al–4V implants by CSD using titanium-isopropoxide chelated by acetylacetone, calcium nitrate and phosphoric acid, as starting materials. Ti/HAP solutions with variable HAP contents ranging from 0 to 100% at 10% intervals were spin-coated onto substrate and prefired at 500 °C. XRD and FE-SEM analysis showed that Ti/HAP coatings with a dense interface between coating and substrate were obtained by final annealing at 500 °C and higher. As confirmed by measuring variations of the P and Ca concentrations after incubation in SBF the coatings induced surface HAP formation.

## Acknowledgements

This work was supported by grant No. 1999-2-31400-003-3 from the Basic Research Program of the Korea Science and Engineering Foundation.

## References

[1] K. De Groot, Bioceramics consisting of calcium phosphate salt, Biomaterials 1 (1980) 47–50.
[2] H.W. Denissen, K. De Groot, P.C. Makkes, A. Hoff, P.J. van den Klopper, Tissue response to dense apatite implants in rats, J. Biomed. Mater. Res. 14 (1980) 713–721.
[3] D. McConnel, Apatite, Its Crystal Chemistry, Mineralogy, Utilization and Geologic and Biologic Occurrences, Springer, New York, 1973, pp. 18–20.
[4] W. Weng, J.L. Baptista, Sol-gel derived porous hydroxyapatite coatings, J. Mater. Sci.: Mater. in Med. 9 (1998) 159–163.
[5] K. Dijk, H.G. Schaeken, J.C.G. Wolke, C.H.M. Mare, F.H.P.M. Habraken, J. Verhoeven, J.A. Jansen, Influence of discharge power level on the properties of hydroxyapatite films deposited on Ti–6Al–4V with RF magnetron sputtering, J. Biomed. Mater. Res. 29 (1995) 269–276.
[6] J. Chen, W. Tong, Y. Cao, J. Feng, X. Zhang, Effect of atmosphere on phase transformation in plasma sprayed hydroxyapatite coatings during heat treatment, J. Biomed. Mater. Res. 34 (1997) 15–20.
[7] P. Sharrock, G. Bonel, Colour centers in plasma-sprayed hydroxyapatite, Biomaterials 13 (1992) 755–758.
[8] Y. Han, K. Xu, J. Lu, Morphology and composition of hydroxyapatite coatings prepared by hydrothermal treatment on electrodeposited brushite coatings, J. Mater. Sci. Lett.: Mater. in Med. 10 (1999) 243–248.
[9] K. Hwang, J. Song, B. Kang, Y. Park, Sol-gel derived hydroxyapatite films on alumina substrates, Surf. Coat. Technol. 123 (2000) 252–255.
[10] K. Hwang, Y. Lim, Chemical and structural changes of hydroxyapatite films by using a sol-gel method, Surf. Coat. Technol. 115 (1999) 172–175.
[11] H. Ji, C.B. Ponton, P.M. Marquis, Microstructural characterization of hydroxyapatite coating on titanium, J. Mater. Sci.: Mater. in Med. 3 (1992) 283–287.
[12] Y. Abe, T. Kokubo, T. Yamamoto, Apatite coating on ceramics, metals and polymers utilizing a biological process, J. Mater. Sci.: Mater. in Med. 1 (1990) 223–238.
[13] W. Neuman, M. Neuman, The Chemical Dynamics of Bone Minerals, University of Chicago, Chicago, IL, 1958, p. 34.